

Polyvinylpyrrolidone-assisted Solvothermal Synthesis of Porous LaCoO₃ Nanospheres as Supercapacitor Electrode

Yazhou Guo¹, Tianyan Shao¹, Huihui You¹, Sheng Li¹, Chao Li¹, Lei Zhang^{1,2*}

¹ School of Chemical Engineering and Technology, Tianjin University, Tianjin 300350, China

² Collaborative Innovation Center of Chemical Science and Engineering (Tianjin), Tianjin 300072, China

*E-mail: zll@tju.edu.cn

Received: 29 April 2017 / Accepted: 6 June 2017 / Published: 12 July 2017

A polyvinylpyrrolidone (1-ethenylpyrrolidin-2-one or PVP)-assisted solvothermal method has been developed to synthesize porous LaCoO₃ nanospheres. Appropriate PVP addition may effectively prohibit the growth of nanospheres and plays an important role in reducing the size of LaCoO₃. The porous morphology of LaCoO₃ nanospheres can be obtained by an annealing process to achieve a specific capacitance of 203 F g⁻¹ at a current density of 1 A g⁻¹ with good cyclic stability for LaCoO₃ which has been prepared with 0.5 g PVP. This attributes to the synergistic effect of both size reduction and porous morphology.

Keywords: perovskite; porous; LaCO₃ nanospheres; supercapacitor; polyvinylpyrrolidone

1. INTRODUCTION

In recent years, transition metal oxides (TMOs) have attracted much attention as electrode materials for use as supercapacitors due to their multiple oxide states, rapid reversible Faradaic surface reaction and satisfactory electrochemical stability [1-4]. LaMnO₃ as one of a number of typical TMOs with perovskite structure has recently been developed and investigated as a pseudocapacitor electrode, and an anion-based fast-charge electrical storage mechanism has been introduced [5]. Similarly, LaCoO₃ possessing the crystalline structure of rhombohedral R-3c may be adopted as an electrode material for supercapacitor [6, 7]. Although an unaggregated spherical oxide with a nanometer-size distribution is the most desirable state for improved capacitance, it is difficult to obtain spherical nanopowder particles through hydrothermal synthesis due to the formation behavior of perovskite [8]. A surfactant such as polyvinylpyrrolidone (1-ethenylpyrrolidin-2-one or PVP) is normally used to modify materials' morphology and microstructure [9]. PVP is a polar molecule and binds very well to

other polar molecules [10, 11]. PVP can be used in hydrothermal synthesis, as a stabilizing agent to prevent the aggregation of metal particles and retain a uniform colloidal dispersion [12].

In this work, porous LaCoO_3 nanospheres have been successfully synthesized by a solvothermal method under the assistance of PVP. The addition of PVP can effectively reduce the size of LaCoO_3 nanospheres, and the uniform distribution of ~ 300 nm LaCoO_3 nanospheres have been obtained using 0.5 g PVP. The size reduction of LaCoO_3 by adding 0.5 g PVP leads to enhanced electrochemical performance and a specific capacitance of 203 F g^{-1} has been achieved at a current density of 1 A g^{-1} with good cyclic stability.

2. EXPERIMENTAL

2.1 Preparation of porous LaCoO_3 nanospheres

The precursor to LaCoO_3 was prepared with a single-step solvothermal method. One mmol of cobalt (II) nitrate hexahydrate (98%, ACS reagent) and 1 mmol of lanthanum (III) nitrate hexahydrate (99.9%-La, REO) were dissolved in a mixture of 160 ml isopropyl alcohol and 32 ml glycerin and stirred for half an hour. Various aliquots of PVP (average molecular mass of 8000) at 0.5 g and 1g were added to the solution along with a sample without PVP for comparison. The mixed solution was transferred into a stainless steel autoclave and heated at 180°C for 6 h. The obtained product was washed three times prior to centrifuge collection, and then dried at 60°C . The precursor powders were annealed at 600°C for 6 h in a pure O_2 atmosphere.

2.2 Materials characterization

The samples' morphology was determined by using a Hitachi S4800 (Japan) scanning electron microscopy (SEM) with a 5.0 kV accelerating voltage. Transmission electron microscopy (TEM) characterization was done using a JEM 3100 (JEOL, Japan) operated at 200 kV. X-ray diffraction (XRD) patterns were accomplished using a Bruker D8 (Cu $\text{K}\alpha$ radiation $\lambda=1.54056 \text{ \AA}$). Cycling voltammetry (CV) and chronopotentiometry (CP) were performed using a CHI660D (Shanghai Chenhua, China) electrochemical workstation.

2.3 Electrochemical measurements

The work electrode slurry was prepared by mixing annealed LaCoO_3 , carbon black (Super P) and polytetrafluoroethylene (binder) at a mass ratio of 8:1:1. The mixed slurry was pasted onto Ni foam with 2 mg cm^{-2} , followed by vacuum dessication at 80°C . The electrochemical measurement was performed using a traditional three-electrode system at room temperature with platinum foil as the counter electrode and Hg/HgO as the reference electrode in an aqueous 6 M KOH electrolyte. The CV curves were measured in a potential range of 0-0.5V vs Hg/HgO and CP was measured in a potential range of 0-0.45V vs Hg/HgO. The cyclic performance was conducted with LAND (Wuhan, China).

3. RESULTS AND DISCUSSION

The XRD patterns (Fig. 1A) shows the crystalline structure of LaCoO_3 prepared with 0, 0.5 and 1 g PVP, respectively. All of the reflections can be readily indexed to rhombohedral LaCoO_3 (JCPDS No. 48-0123) while no other phase can be detected. This indicates that the LaCoO_3 single phase has been achieved successfully after annealing at 600°C for 6 h in an O_2 atmosphere, and the phase purity is not affected by the addition of PVP.

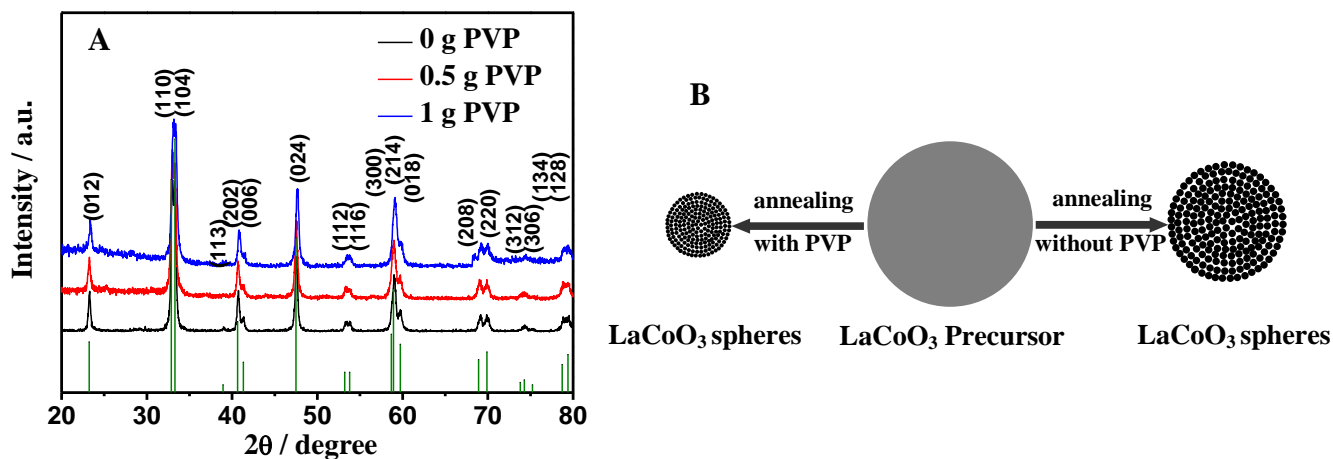


Figure 1. XRD patterns of LaCoO_3 prepared with various amounts of PVP (A), Schematic illustration for the formation of porous LaCoO_3 nanospheres (B).

The microstructures of LaCoO_3 precursor and LaCoO_3 annealed for 6 h in O_2 are revealed by SEM. The as-prepared LaCoO_3 precursor without PVP (Fig. 2A) consists of uniform micro-spheres with diameters of $\sim 1 \mu\text{m}$. The spherical morphology is well maintained after annealing (Fig. 2B), however, the diameters of the spheres are reduced to $\sim 500 \text{ nm}$ because of the shrinkage during annealing. The surface roughness of the spheres becomes more significant after annealing, suggesting that the spheres might be composed of LaCoO_3 nanoparticles. By adding 0.5 g of PVP, the morphology of most LaCoO_3 nanospheres is retained with a dramatic reduction in their average size to $\sim 300 \text{ nm}$ after annealing (Fig. 2C). The size of LaCoO_3 is reduced further by increasing the amount of PVP to 1 g, however, the spherical structure can not be retained and tends to deteriorate, leading to the collapse of the LaCoO_3 nanospheres (Fig. 2D). TEM images (Fig. 2E, F) clearly demonstrate that the porous morphology of the LaCoO_3 nanospheres after annealing and the porous structure is not affected by the addition of 0.5 g PVP. As illustrated in Fig. 1B, the formation of porous LaCoO_3 nanospheres may be attributed to the annealing process of the LaCoO_3 precursor, with which the nucleation and growth of LaCoO_3 nanoparticles continues during annealing, eventually forming the porous nanospheres. The physical absorption of PVP on the nanoparticles surface may prohibit the nanospheres' growth. Therefore, PVP is used here as an important agent in reducing the size of LaCoO_3 [13-15]. It is important to note that from the cavity of the broken parts in Fig. 2D, the LaCoO_3 nanospheres obtained might be hollow inside.

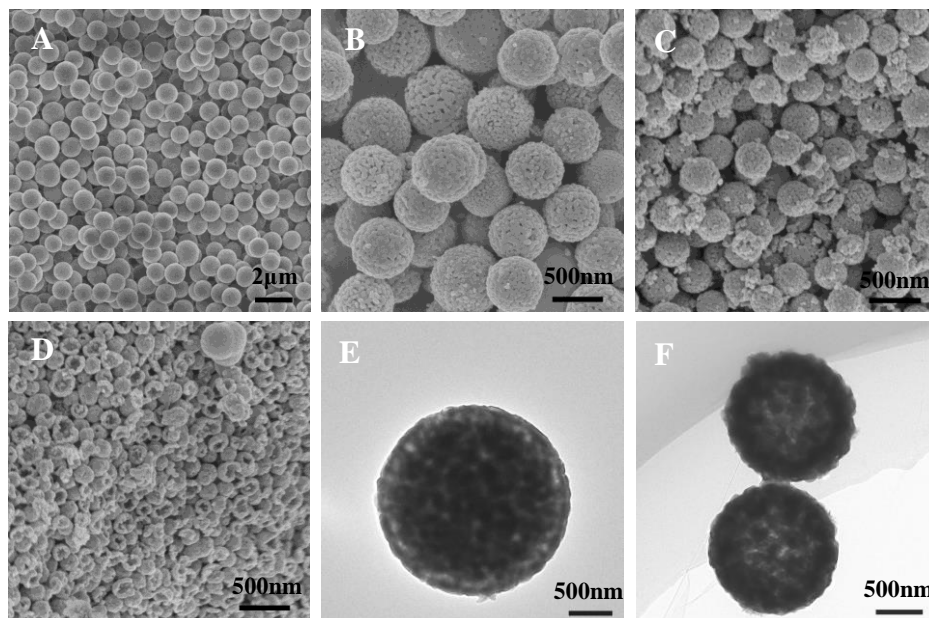


Figure 2. SEM images of LaCoO_3 precursor prepared without PVP (A), LaCoO_3 prepared with 0 (B), 0.5 (C), 1 g (D) PVP after annealing, TEM images of porous LaCoO_3 nanospheres prepared with 0 (E), 0.5 (F) g PVP after annealing.

Fig. 3A shows the cyclic voltammetry (CV) tested in 0-0.5 V at a scanning rate of 10 mV s^{-1} for LaCoO_3 prepared with 0, 0.5 and 1 g PVP respectively. All the samples display distinct redox peaks during the anodic and cathodic sweeps, showing characteristics of the electrochemical supercapacitors delivering reversible capacitance based on the surface reactions [16, 17]. LaCoO_3 prepared with 0.5 g PVP demonstrates the largest area enclosed under the CV curve, indicating the greatest specific capacitance. The chronopotentiometry (CP) measurements are performed in the 0-0.45 V voltage range at a charging-discharging current of 1 A g^{-1} (Fig. 3B). LaCoO_3 prepared with 0.5 g PVP exhibits the longest charging and discharging duration, indicating the excellent electrochemical performance of the porous LaCoO_3 nanospheres. Fig. 3C shows specific capacitances as a function of current densities of LaCoO_3 prepared with various additions of PVP. It reveals that LaCoO_3 prepared with 0.5 g PVP exhibits the highest specific capacitance of 203 F g^{-1} at a current density of 1 A g^{-1} and a capacitance as high as 123 F g^{-1} can be achieved at a current density of 20 A g^{-1} . This performance is comparable to perovskite such as $\text{La}_{0.85}\text{Sr}_{0.15}\text{MnO}_3$ [19] and double perovskite Y_2NiMnO_6 [20] and it could be further optimized by controlled doping on the B-site of the perovskite structure [21-22] (Table. 1). However, LaCoO_3 prepared with 0 and 1 g PVP show a capacitances reduction of 51.7 and 162 F g^{-1} at a current density of 1 A g^{-1} , and 11.5 and 88.4 F g^{-1} at a current density of 20 A g^{-1} , respectively. The cyclic stability of porous LaCoO_3 nanospheres is evaluated by repeated charging and discharging for 5000 cycles at a current density of 1 A g^{-1} (Fig. 3D). The specific capacitance increases slightly from 203 F g^{-1} to 225 F g^{-1} during the first 200 cycles, which might be due to electrochemical activation [18].

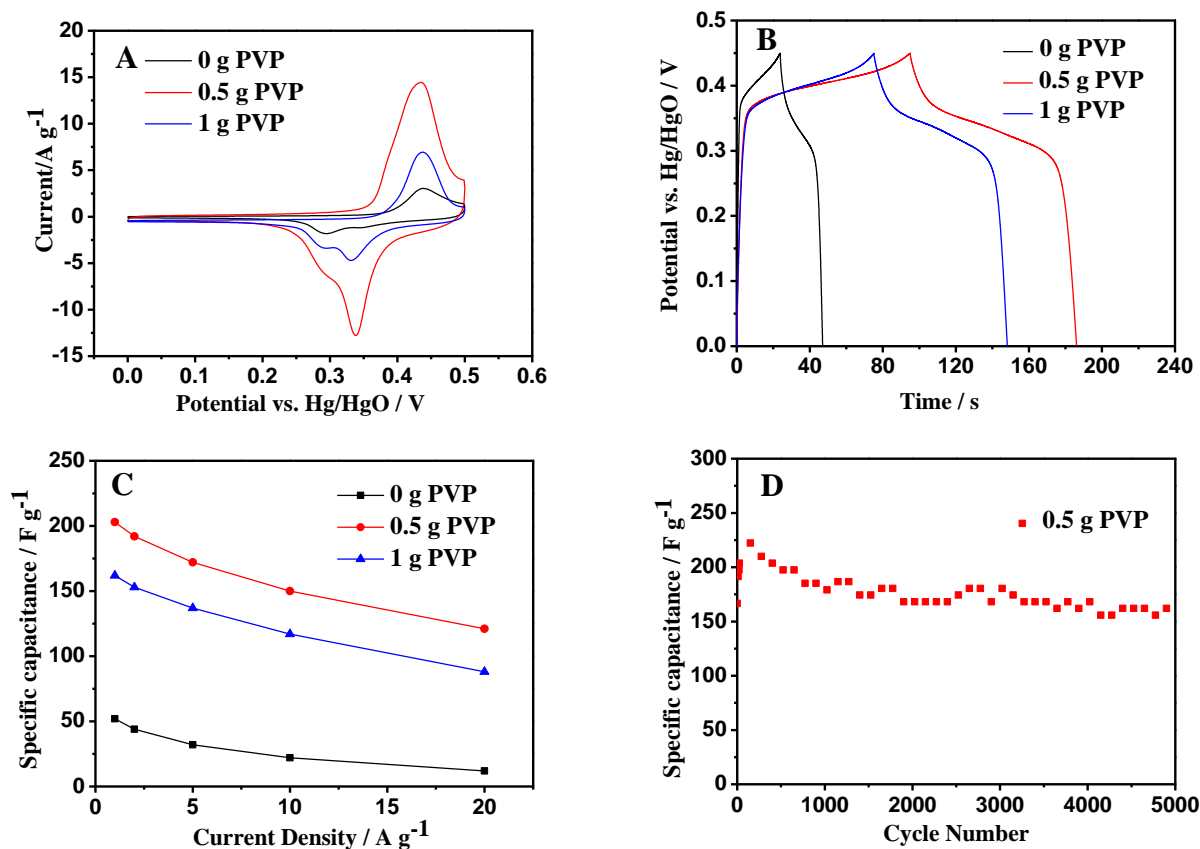


Figure 3. CV curves of LaCoO₃ electrodes prepared with various additions of PVP at a scanning rate of 10 mV s⁻¹ (A), charge-discharge curves at a current density of 1 A g⁻¹ (B), specific capacitance as a function of current density (C), cyclic performance of LaCoO₃ prepared with 0.5 g PVP at a current density of 1 A g⁻¹ (D).

Table 1. Performances comparison of some perovskite oxides as supercapacitor electrodes.

Perovskite oxides	Specific capacitance	Electrolyte
La _{0.85} Sr _{0.15} MnO ₃ [19]	198 F g ⁻¹ at 0.5 A g ⁻¹	aqueous KOH
Y ₂ NiMnO ₆ [20]	77.76 F g ⁻¹ at 30 mA g ⁻¹	aqueous KOH
SrCo _{0.9} Nb _{0.1} O _{3-δ} [21]	773.6 F g ⁻¹ at 0.5 A g ⁻¹	aqueous KOH
Ba _{0.5} Sr _{0.5} Co _{0.8} Fe _{0.2} O _{3-δ} [22]	572 F g ⁻¹ at 1 A g ⁻¹	aqueous KOH
porous LaCoO ₃ in this work	203 F g ⁻¹ at 1 A g ⁻¹	aqueous KOH

Porous LaCoO_3 nanospheres demonstrate good specific capacitance and cyclic performance due to the synergistic effect of porous morphology and size reduction. On one hand, the porous structure significantly improves ionic and electronic transfer, which is beneficial to rapid ion and electron transfer, leading to enhanced electrochemical performance. On the other hand, the size reduction of LaCoO_3 caused by the addition of PVP might provide more active sites to produce the electrochemical reaction due to an increase in specific surface area. EIS measurements (Fig. 4) further confirm that porous LaCoO_3 nanospheres with reduced size exhibit the smallest real axis intercept (merely 0.375Ω) and a negligible semicircle, indicating the lowest recorded internal resistance and charge transfer resistance.

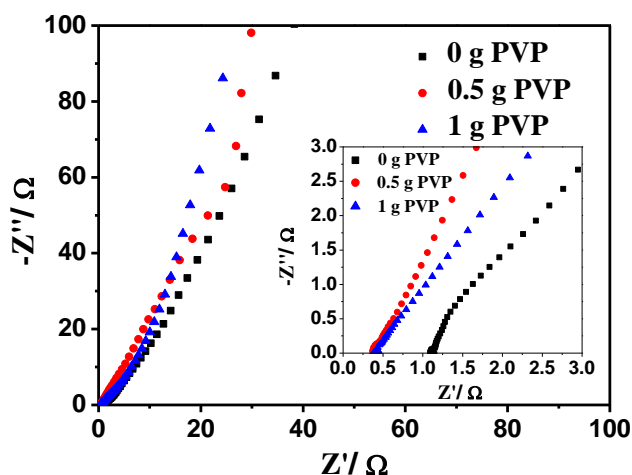


Figure 4. Electrochemical impedance spectroscopies of LaCoO_3 prepared with various aliquots of PVP.

CONCLUSIONS

We have successfully utilized PVP as a promising agent in solvothermal synthesis to obtain porous LaCoO_3 nanospheres. The proper utilization of PVP can significantly reduce the size of LaCoO_3 with maintaining its spherical structure, and this porous morphology can be obtained by the annealing process. Electrochemical measurements indicate that porous LaCoO_3 nanospheres manifest promising electrode for application as supercapacitors with satisfactory capacitance and cyclic stability. The results of this work will hopefully propagate the design of other porous oxides in various applications.

ACKNOWLEDGEMENTS

This work was financially supported by the National Natural Science Foundation of China (Grant Nos. 21406161, 21611130172).

References

1. Y. Li, H. Xie, J. Wang and L. Chen, *Mater. Lett.*, 65 (2011) 403.
2. N. Wang, M. Q. Yao, P. Zhao, W. C. Hu and S. Komarneni, *J. Mater. Chem. A.*, 5 (2017), 5838.
3. X. G. Li, L. Wang, J. H. Shi, N. X. Du and G. H. He, *ACS Appl. Mater. Interfaces.*, 8 (2016) 17276.
4. L. F. Shen, L. Yu, H. B. Wu, X. Y. Yu, X. G. Zhang and X. W. Lou, *Nat. Commun.*, 6 (2015) 6694.
5. J. T. Mefford, W. G. Hardin, S. Dai, K. P. Johnston and K. J. Stevenson, *Nat. Mater.*, 13 (2014) 726.
6. V. V. Kharton, F. M. Figueiredo, A. V. Kovalevsky, A. P. Viskup, E. N. Naumovich, A. A. Yaremchenko, I. A. Bashmakov and F. M. B. Marques, *J. Eur. Ceram. Soc.*, 21 (2001) 2301.
7. M. S. D. Read, M. S. Islam, G. W. Watson, F. King and F. E. Hancock, *J. Mater. Chem.*, 10 (2000) 2298.
8. J. Y. Choi, C. H. Kim and D. K. Kim, *J. Am. Ceram. Soc.*, 81 (1998) 1353.
9. F. Wang, J. Liu, J. Kong, Z. Zhang and X. Wang, *J. Mater. Chem.*, 21 (2011) 4314.
10. I. P. Santos and L. M. Liz-Marzan, *Langmuir*, 18 (2002) 2888.
11. Y. Sun and Y. Xia, *Science*, 298 (2002) 2176.
12. N. Yu, L. Kuai, Q. Wang and B. Geng, *Nanoscale*, 4 (2012) 5386.
13. S. H. Xuan, F. Wang, Y. X. J. Wang, J. C. Yu and K. C. F. Leung, *J. Mater. Chem.*, 20 (2010) 5086.
14. T. He, D. Chen and X. L. Jiao, *Chem. Mater.*, 16 (2004) 737.
15. X. Yao and H. C. Zeng, *J. Phys. Chem. C.*, 111, (2007) 13301.
16. G. Wang, D. Cao, C. Yin, Y. Gao, J. Yin and L. Cheng, *Chem. Mater.*, 21 (2009) 5112.
17. G. Wang, L. Zhang and J. Zhang, *Chem. Soc. Rev.*, 41 (2012) 797.
18. C. C. Hu, K. H. Chang and T. Y. Hsu, *J. Electrochem. Soc.*, 155 (2008) F196.
19. X. W. Wang, Q. Q. Zhu, X. E. Wang, H. C. Zhang, J. J. Zhang and L. F. Wang, *J. Alloy. Compd.*, 675 (2016) 195.
20. M. Alam, K. Karmakar, M. Pal and K. Mandal, *RSC Adv.*, 6 (2016) 114722.
21. L. Zhu, Y. Liu, C. Su, W. Zhou, M. L. Liu and Z. P. Shao, *Angew. Chem. Int. Edit.*, 55 (2016) 1.
22. Y. Liu, J. Dinh, M. O. Tade and Z. P. Shao, *ACS Appl. Mater. Interfaces.*, 8 (2016) 23774.

© 2017 The Authors. Published by ESG (www.electrochemsci.org). This article is an open access article distributed under the terms and conditions of the Creative Commons Attribution license (<http://creativecommons.org/licenses/by/4.0/>).